THE JOURNAL OF PHYSICAL CHEMISTRY Letters

LETTER

pubs.acs.org/JPCL

Fluid Flow and Effusive Desorption: Dominant Mechanisms of Energy Dissipation after Energetic Cluster Bombardment of Molecular Solids

Daniel A. Brenes, Barbara J. Garrison, and Nicholas Winograd*

Department of Chemistry, The Pennsylvania State University, University Park, Pennsylvania 16802, United States

Zbigniew Postawa

Smoluchowski Institute of Physics, Jagiellonian University, ul. Reymonta 4, 30-059 Krakow, Poland

Andreas Wucher

Faculty of Physics, University of Duisburg-Essen, 47048 Duisburg, Germany

Paul Blenkinsopp

Ionoptika Ltd., Epsilon House, Chilworth Science Park, Southampton SO53 4NF, U.K.

ABSTRACT: The angular distribution of intact organic molecules desorbed by energetic C_{60} primary ions was probed both experimentally and with molecular dynamics computer simulations. For benzo[a]pyrene, the angular distribution of intact molecules is observed to peak at off-normal angles. Molecular dynamics computer simulations on a similar system show the mechanism of desorption involves fast deposition of energy followed by fluid-flow and effusive-type emission of intact molecules. The off-normal peak in the angular distribution is shown to arise from emission of intact molecules from the rim of a crater formed during the cluster impact. This signature is unique for molecules because fragmentation processes remove molecules that would otherwise eject at directions near-normal to the surface.

SECTION: Surfaces, Interfaces, Catalysis

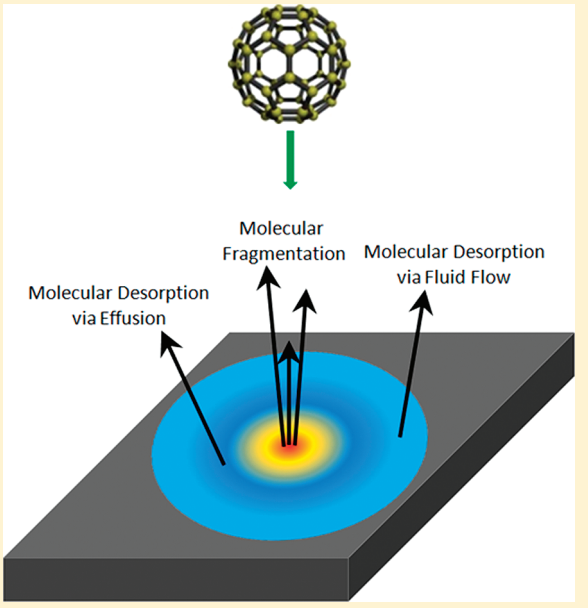

Elucidation of the dynamics of the interaction of energetic particles with solids has been of long-standing fundamental scientific interest. Knowledge about the details of these interactions is important for understanding such diverse phenomena as the doping of semiconductor devices and the shaping of the topography of extraterrestrial surfaces. The emergence of cluster ion sources has expanded the scope of this field even further to include the smoothing and modification of semiconductor surfaces,[1−4] the cleaning of specific polymers,[5] biological mass spectrometry,[6−8] depth profiling of molecular solids,[9−12] and three-dimensional chemical imaging on the nanoscale.[13,14]

The unique nature of the cluster/solid interaction has been elegantly illustrated using molecular dynamics (MD) computer simulations.[1,15−17] A key feature is that the kinetic energy of each incident particle in the cluster is equal to the total energy of the cluster divided by the number of atoms. For 20 keV C_{60}, for example, each C atom imparts only 333 eV into the solid. Since there are a large number of lower energy collisions occurring nearly simultaneously, traditional analytical theories based upon

Received: May 25, 2011
Accepted: July 22, 2011
Published: July 22, 2011

binary collisions in atomic cascades[18] cannot be applied to this situation. The first correction to this approximation focused upon developing nonlinear cascades.[19] However, MD calculations of clusters ranging from Au_3 to C_{60} show an alternative description in which during the initial stages of energy deposition, the dynamics can be approximated by a single large particle impacting the surface.[20,21] Subsequent to the energy deposition by the pseudosingle large particle, a crater of several nanometers in depth and width results from a single impact. The energy is deposited very near the surface, resulting in high sputtering yields and low subsurface damage when compared to other projectiles.

Many aspects of the MD approach have been verified by experiments for elemental solids, but the full simulations are challenging for molecular solids. There are hints, however, of characteristics of molecular ejection due to cluster bombardment from partial MD simulations followed by analytic models. For example, an analytical scheme has been developed that takes advantage of the fluid-like motion exhibited by particles seen in MD studies. This mesoscale energy deposition footprint (MEDF) approach incorporates parameters from MD calculations obtained after just a few tens of femtoseconds and extends the time-prediction to a range where sputtering has ceased.[21] This model has been used successfully to predict yields of molecules when C_{60} bombards water ice[22] and benzene[23] at kinetic energies up to 120 keV. Short-time (1.5 ps) simulations of C_{60} bombardment of octane and octatetraene also indicate that intact molecules flow from the edge of the crater with low internal energies.[24] The proposal of intact emission by a fluid-flow mechanism rather than a traditional energetic sputtering mechanism is worthy of testing.

To elucidate the mechanism of molecular emission due to energetic cluster bombardment, here we experimentally measure the trajectories of energy- and angle-resolved neutral (EARN) molecules desorbed from a molecular solid by 20 keV C_{60} bombardment and compare these trajectories to those calculated on a closely related system by MD computer simulations. This comparison reveals that molecular desorption occurs by two distinct mechanisms. These include a fluid-flow-like process at higher kinetic energies,[21,24] and an effusive-type desorption at lower ejection kinetic energies.[25] It is possible to arrive at this conclusion by examination of the anisotropy associated with the polar angle distribution of the ejected molecules and by a molecular level comparison of these trajectories to those computed by MD using a simplified description of the internal structure of the molecule. Even though different molecules are used in comparing experiment and theory, previous simulations have shown that the mechanism of intact emission is similar, regardless of the specific molecule, under C_{60} bombardment.[22−24,26,27] These findings are important for refining existing models of cluster/solid interactions and for providing guidance to elucidate mechanisms of desorption over a wide time scale.

The EARN distribution of material removed from surfaces by energetic ion beams provides a powerful diagnostic signature that allows the mechanisms responsible for atomic, molecular, and cluster emission to be unraveled. The experimental and calculated kinetic energy distributions are shown in Figure 1. The signal intensities are normalized and plotted as a function of the ratio between the molecule's kinetic energy to the peak emission energy from the distribution. The peak emission energies are 0.63 and 0.21 eV for benzo[a]pyrene (b[a]p) and coarse-grained (cg-) benzene, respectively. The peak in

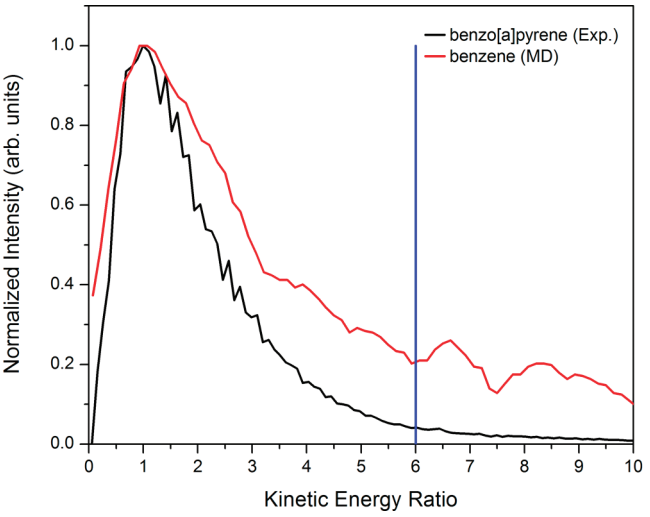

Figure 1. The kinetic energy distribution for neutral intact b[a]p molecules (black line, experiment) and cg-benzene molecules (red line, calculated) desorbed by 20 keV C_{60} primary ions with an impact angle of 0° to the surface normal. The abscissa uses a ratio of the molecule's kinetic energy to the kinetic energy of the peak position, 0.63 eV for b[a]p and 0.21 eV for cg-benzene.

the energy distribution is related to the cohesive energy of the system. Since b[a]p has a cohesive energy ∼2.5 times larger than benzene,[28] these relative peak positions are consistent with this relationship.

The polar angle distributions of ejected molecules are shown in Figure 2 for the experimentally measured neutral b[a]p molecules (Figure 2a) and the calculated cg-benzene molecules (Figure 2b). In both cases, the integrated kinetic energy polar angle distribution is further split into two distributions representing low and high kinetic energy molecules. The dividing energy is indicated by the vertical line shown in Figure 1. The position of this line is selected so as to optimize the anisotropy visible at high kinetic energy. Note that due to differences in the cohesive energy between b[a]p and benzene, the cutoff energy is not the same for both cases.

The polar angle distribution over all kinetic energies exhibits a peak at ∼30° superimposed on an overcosine type background. After resolving the kinetic energy into two regimes, it is clear that the off-normal emission at ∼30° consists mainly of high energy molecules, while the overcosine component is comprised of molecules of low kinetic energy. Experimentally, the polar angle distributions are unique since off-normal emission has not previously been predicted or measured within the keV energy regime of medium-sized cluster projectiles. The polar angle distributions for atoms from an amorphous or polycrystalline metal and organic molecules under atomic bombardment have been experimentally measured to be overcosine,[29−32] and for atoms to be near cosine for Au_2 and Au_3 cluster bombardment.[32] Only in the case of very large clusters such as Ar_{2000} and Ar_{3000} have off-normal emission angles been measured for atomic systems.[2−4,33] The mechanism for this case is lateral sputtering of material due to a blockade from the cluster, a mechanism not applicable to medium-sized clusters such as C_{60}.

The mechanisms giving rise to the two main features in Figure 2a,b can be discerned from the MD simulations and then used to interpret the experimental results. To begin, vector plots

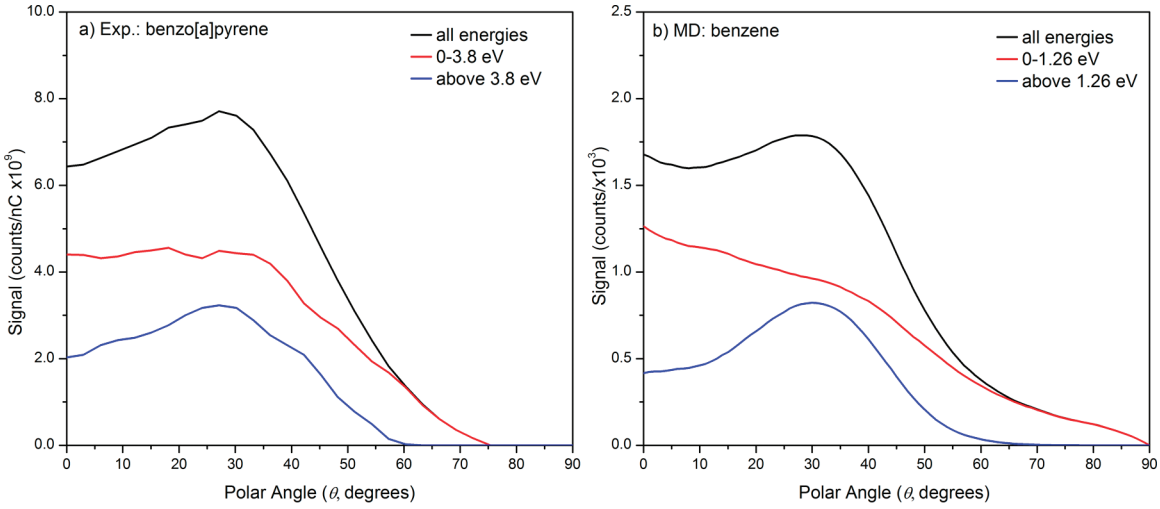

Figure 2. The polar angle distribution of organic molecules desorbed by 20 keV C_{60} primary ions. The molecular signal intensity is plotted versus the emission angle and as a function of emission energy: (a) measured b[a]p molecules with all energies (black line), 0−3.8 eV (red line), and above 3.8 eV (blue line), and (b) calculated cg-benzene molecules with all energies (black line), 0−1.26 eV (red line), and above 1.26 eV (blue line).

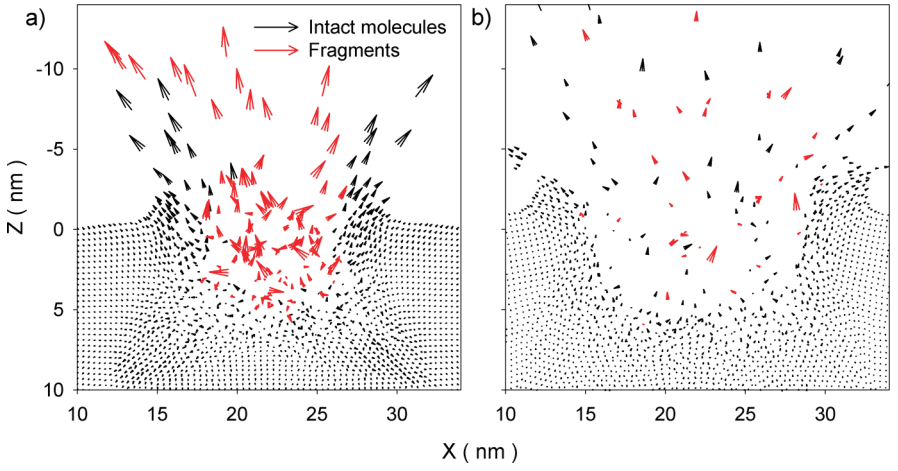

Figure 3. Time snapshots from the MD computer simulations of the emission of cg-benzene molecules (black) and fragments (red) represented as a vector plot at (a) 2 ps and (b) 8 ps upon C_{60} impact. The vector tail depicts the particle's position at the given time, while the vector head depicts its position 0.3 ps later. The direction of the vector indicates the particle's emission angle and/or lateral relocation, while the length corresponds to its kinetic energy.

are shown in Figure 3 for times of 2 and 8 ps after the impact illustrating the direction of motion for cg-benzene molecules and fragments as the crater develops. The tail of the vector is the position of the species (molecule or fragment) at the given time, and the head of the vector is the position 0.3 ps later. The length of the vector corresponds to the velocity, and the angle corresponds to the direction of motion. In the 2 ps snapshot, the kinetic energies of the ejecting cg-benzene molecules tend to be greater than 2 eV, and the molecules are primarily emitted from the edges of the crater, reflecting the off-normal peak for the polar angle distribution of intact cg-benzene molecules shown in Figure 2b. Note that only fragments are emitted along the surface normal and are confined to a region that is centralized around the point of impact. The 8 ps snapshot shows a fully developed crater in which both cg-benzene molecules and fragments with kinetic energies less than 1 eV are moving with motions that emit at various polar angles giving rise to the overcosine shape in Figure 2b.

The molecular emission angles can be understood based on the physics of the motion that is initiated following the C_{60} impact. Upon impact, C_{60} swiftly penetrates and disintegrates into carbon atoms while depositing its kinetic energy in less than 100 fs in the top 2−3 nm, creating an energized region that is mostly composed of fragments. The energized region plays two roles in the emission of molecules. The first role is that it expands outward into the surrounding intact molecules, which ultimately begin to develop a crater. During the expansion, the energized region laterally pushes on adjacent molecules causing an upward sweeping motion of intact molecules that initiates the emission of molecules from the surface at off-normal angles. Previous studies have described the sweeping motion to follow the concepts of fluid dynamics in which material flows from the surface into vacuum with fluid-like motions. In this simulation, the motion of the emitted molecules matches those from previous simulations[21−24] and therefore can be characterized

dx.doi.org/10.1021/jz200708j |J. Phys. Chem. Lett. 2011, 2, 2009–2014

as molecular emission by fluid flow. The second role the energized region plays is related to the emission of fragments. As the energized region expands, there are collisions between the carbon atoms from the disintegrated C_{60} cluster and fragments that cause the emission of fragments along the surface normal. Since the region is composed mainly of fragments, very few intact molecules are able to eject along the surface normal. For atomic solids, these energetic particles emitted in a normal direction would be the same as those emitted off-normal, and the angular distribution would appear as overcosine. In fact, if all ejected material is counted instead of only intact molecules, we find the angular distribution to be overcosine. Therefore, the appearance of the off-normal peak in molecular ejection is caused by the fragmentation of molecules that are emitted in the direction normal to the surface. Finally, once the expansion of the energized region is completed, the crater is fully developed, and the fluid-like motions cease, but the emission of intact molecules and fragments continue due to effusive-type motions.[25] At this point, only interactions between weakly bound fragments and intact molecules along the walls of the fully developed crater can occur. These interactions cause an effusive-type desorption of weakly bound intact molecules with very low kinetic energies and emission angles that are overcosine. In fact, there are molecules seen in the vector plots that eject directly from beneath the impact region.

One issue is whether there is a significant difference between the experimental system of b[a]p and the computational system of cg-benzene. First, the fact that the energy-resolved angular distributions show similar characteristics without any fitting of the calculation to the experiment suggests that the essential physics in the two systems is similar. Second, for the emission due to fluid flow, the only significant difference between the different systems is the relative number of molecules ejected.[21,22,24] The simulations show that the volume of material that flows from the system is similar. Hence, more intact molecules of benzene are expected to be emitted because of their smaller size. All molecules desorbed by fluid flow should have low internal energies and are not expected to fragment. Third, for the effusive mechanism, we expect more of the larger b[a]p to be damaged and more of the intact benzene molecules to eject. None of these considerations, however, lead one to conclude that the essential physics of emission of b[a]p should be different from that of benzene. Moreover, we have focused on only the major features of the energy-resolved angular distributions and not on small differences such as the local maximum of the total polar distribution of benzene in the normal direction.

In summary, we have shown from a collective experimental and theoretical approach that the emission of organic molecules induced by C_{60} primary ions is characterized by a fast deposition of energy at the surface followed by desorption that exhibits fluid-like and effusive-type motions. In the early stages of emission, an energized region composed predominantly of molecular fragments is created. Expansion of this region initiates the ejection of fast moving intact molecules with fluid-like motions that lead to off-normal emission angles. The appearance of the off-normal peak arises due to lack of molecules that would otherwise eject in the near-normal direction but are fragmented instead. At later times, slow moving molecules are desorbed by effusive-type motions, causing emission angles broadly peaked about the surface normal. This vision of molecular desorption affirms the fundamental basis of the MEDF model and offers new opportunities for developing analytical theories that span multiple time domains.

EXPERIMENTAL DETAILS

The experiments were conducted in a unique time-of-flight mass spectrometer which utilizes a gated, position sensitive microchannel plate detector to collect EARN-particle distributions for material desorbed from ion bombarded surfaces. Although details of the EARN mass spectrometer can be found elsewhere,[34] a brief description is highlighted. The EARN is equipped with a fullerene ion source (Ionoptika, Ltd.) capable of delivering 25 nA of C_{60}^+ ions accelerated to 20 keV. A 200 ns pulse of C_{60}^+ ions was used to bombard at normal incidence a 400 nm film of b[a]p, $C_{20}H_{12}$ (Aldrich Chemical Co.). This molecule was chosen since the film could be prepared by physical vapor deposition[35] resulting in a pure amorphous molecular film with a uniform thickness large enough to avoid substrate effects. Moreover, the photoionization cross section is large enough to achieve the necessary sensitivity and the rigidity of the molecule lessens the probability of photodissociation.[29,36−38] Thickness was monitored using a quartz crystal microbalance (TM-400, Maxtek, Inc.) and verified with an atomic force microscope (Nanopics 2100, TLA Tencor, Inc.) to be 400 nm with a surface roughness of 2 nm rms. A Nd:YAG-pumped dye laser (Lambda-Physik ScanMate Pro) producing 280 nm[36] of light with 6 ns pulses and focused into a ribbon shape with peak power densities of 2×10^5 W/cm^2 was employed to intersect and photoionize the sputtered neutral flux. The kinetic energy and polar angle distributions were measured by recording the mass-selected signal amplitude for b[a]p as a function of position on the detector and time delay between the C_{60} impact and photoionization event. To minimize the photoionization of gas phase molecules and previously observed thermal effects in molecular sputtering,[39,40] the b[a]p film was held at 85 K throughout the experiment. Any interfering background signals were recorded and subtracted for each time delay.

COMPUTATIONAL DETAILS

MD calculations were performed using 20 keV C_{60} projectiles to bombard at normal incidence a benzene crystal arranged in a hemispherical shape with a radius of 25.7 nm. A heat bath composed of rigid and stochastic molecules is employed to maintain a temperature of 0 K and prevent the reflection of C_{60}-induced pressure waves from the boundaries. This choice of model system for comparison to experiment was constrained by a number of factors. First, this system has been optimized for computational efficiency by implementation of a coarse-graining approximation. This method provides an approach to understanding molecular fragmentation by combining hydrogen atoms with their nearest-bonded carbon atom into a bead identified as CH.[41] Second, for the simulations, it is desirable to utilize a smaller molecule since there will be a higher intact molecular yield needed to obtain statistically significant energy and angular distributions.

AUTHOR INFORMATION

Corresponding Author

*Phone: 814-863-0001. Fax: 814-863-0618. E-mail: nxw@psu.edu.

■ ACKNOWLEDGMENT

The authors gratefully acknowledge financial support from the National Institute of Health Grant No. 2R01 EB002016-18, the National Science Foundation Grant Nos. CHE-0908226 and CHE-0910564, the Department of Energy Grant No. DE-FG02-06ER15803, and the Polish Ministry of Science and Higher Education Program No. N N204 183940.

■ REFERENCES

(1) Yamada, I.; Matsuo, J.; Insepov, Z.; Akizuki, M. Surface Modifications by Gas Cluster Ion Beams. *Nucl. Instrum. Methods Phys. Res., Sect. B* **1995**, *106*, 165–169.

(2) Toyoda, N.; Matsui, S.; Yamada, I. Ultra-Smooth Surface Preparation Using Gas Cluster Ion Beams. *Jpn. J. Appl. Phys., Part 1* **2002**, *41*, 4287–4290.

(3) Toyoda, N.; Kitani, H.; Hagiwara, N.; Matsuo, J.; Yamada, I. Surface Smoothing Effects with Reactive Cluster Ion Beams. *Mater. Chem. Phys.* **1998**, *54*, 106–110.

(4) Toyoda, N.; Matsuo, J.; Yamada, I. Surface Modification with Gas Cluster Ion Beams from Fundamental Characteristics to Applications. *Nucl. Instrum. Methods Phys. Res., Sect. B* **2004**, *216*, 379–389.

(5) Sanada, N.; Yamamoto, A.; Oiwa, R.; Ohashi, Y. Extremely Low Sputtering Degradation of Polytetrafluoroethylene by C_{60} Ion Beam Applied in XPS Analysis. *Surf. Interface Anal.* **2004**, *36*, 280–282.

(6) Lanekoff, I.; Kurczy, M. E.; Hill, R.; Fletcher, J. S.; Vickerman, J. C.; Winograd, N.; Sjovall, P.; Ewing, A. G. Time of Flight Mass Spectrometry Imaging of Samples Fractured In Situ with a Spring-Loaded Trap System. *Anal. Chem.* **2010**, *82*, 6652–6659.

(7) Kurczy, M. E.; Piehowsky, P. D.; Willingham, D.; Molyneaux, K. A.; Heien, M. L.; Winograd, N.; Ewing, A. G. Nanotome Cluster Bombardment to Recover Spatial Chemistry After Preparation of Biological Samples for SIMS Imaging. *J. Am. Soc. Mass. Spectrom.* **2010**, *21*, 833–836.

(8) Jones, E. A.; Lockyer, N. P.; Vickerman, J. C. Depth Profiling Brain Tissue Sections with a 40 keV C_{60}^+ Primary Ion Beam. *Anal. Chem.* **2008**, *80*, 2125–2132.

(9) Winograd, N. The Magic of Cluster SIMS. *Anal. Chem.* **2005**, *77*, 142a–149a.

(10) Cheng, J.; Wucher, A.; Winograd, N. Molecular Depth Profiling with Cluster Ion Beams. *J. Phys. Chem. B* **2006**, *110*, 8329–8336.

(11) Mahoney, C. M.; Roberson, S. V.; Gillen, G. Depth Profiling of 4-Cetamindophenol-Doped Poly(lactic acid) Films Using Cluster Secondary Ion Mass Spectrometry. *Anal. Chem.* **2004**, *76*, 3199–3207.

(12) Shard, A. G.; Green, F. M.; Brewer, P. J.; Seah, M. P.; Gilmore, I. S. Quantitative Molecular Depth Profiling of Organic Delta-Layers by C_{60} Ion Sputtering and SIMS. *J. Phys. Chem. B* **2008**, *112*, 2596–2605.

(13) Fletcher, J. S.; Lockyer, N. P.; Vaidyanathan, S.; Vickerman, J. C. ToF-SIMS 3D Biomolecular Imaging of Xenopus Laevis Oocytes Using Buckminsterfullerene C_{60} Primary Ions. *Anal. Chem.* **2007**, *79*, 2199–2206.

(14) Wucher, A.; Cheng, J.; Winograd, N. Protocols for Three-Dimensional Molecular Imaging Using Mass Spectrometry. *Anal. Chem.* **2007**, *79*, 5529–5539.

(15) Yamada, I.; Matsuo, J.; Toyoda, N.; Kirkpatrick, A. Materials Processing by Gas Cluster Ion Beams. *Mater. Sci. Eng., R* **2001**, *34*, 231–295.

(16) Garrison, B. J.; Postawa, Z. Computational View of Surface Based Organic Mass Spectrometry. *Mass Spectrom. Rev.* **2008**, *27*, 289–315.

(17) Urbassek, H. M. Results of Molecular Dynamics Calculations. In *Sputtering by Particle Bombardment*; Behrisch, R., Eckstein, W., Eds.; Springer: Berlin, 2007; Vol. 110, pp 189−230.

(18) Sigmund, P. Theory of Sputtering. I. Sputtering Yield of Amorphous and Polycrystalline Targets. *Phys. Rev.* **1969**, *184*, 383–&.

(19) Sigmund, P.; Claussen, C. Sputtering from Elastic-Collision Spikes in Heavy-Ion-Bombarded Metals. *J. Appl. Phys.* **1981**, *52*, 990–993.

(20) Ryan, K. E.; Russo, M. F.; Smiley, E. J.; Postawa, Z.; Garrison, B. J. Friction Model to Describe Cluster Bombardment. *Appl. Surf. Sci.* **2008**, *255*, 893–896.

(21) Russo, M. F.; Garrison, B. J. Mesoscale Energy Deposition Footprint Model for Kiloelectronvolt Cluster Bombardment of Solids. *Anal. Chem.* **2006**, *78*, 7206–7210.

(22) Russo, M. F.; Szakal, C.; Kozole, J.; Winograd, N.; Garrison, B. J. Sputtering Yields for C_{60} and Au_3 Bombardment of Water Ice as a Function of Incident Kinetic Energy. *Anal. Chem.* **2007**, *79*, 4493–4498.

(23) Ryan, K. E.; Garrison, B. J. Cluster Size Dependence and Yield Linearity in Cluster Bombardment Simulations of Benzene. *Anal. Chem.* **2008**, *80*, 6666–6670.

(24) Garrison, B. J.; Postawa, Z.; Ryan, K. E.; Vickerman, J. C.; Webb, R. P.; Winograd, N. Internal Energy of Molecules Ejected Due to Energetic C_{60} Bombardment. *Anal. Chem.* **2009**, *81*, 2260–2267.

(25) Colla, T. J.; Aderjan, R.; Kissel, R.; Urbassek, H. M. Sputtering of Au (111) Induced by 16-keV Au Cluster Bombardment: Spikes, Craters, Late Emission and Fluctuations. *Phys. Rev. B* **2000**, *62*, 8487–8493.

(26) Delcorte, A.; Garrison, B. J. Sputtering Polymers with Buckminsterfullerene Projectiles: A Coarse-Grain Molecular Dynamics Study. *J. Phys. Chem. C* **2007**, *111*, 15312–15324.

(27) Paruch, R.; Rzeznik, L.; Czerwinski, B.; Garrison, B. J.; Winograd, N.; Postawa, Z. Molecular Dynamics Simulations of Sputtering of Langmuir−Blodgett Multilayers by Kiloelectronvolt C_{60} Projectiles. *J. Phys. Chem. C* **2009**, *113*, 5641–5648.

(28) Roux, M. V.; Temprado, M.; Chickos, J. S.; Nagano, Y. Critically Evaluated Thermochemical Properties of Polycyclic Aromatic Hydrocarbons. *J. Phys. Chem. Ref. Data* **2008**, *37*, 1855–1996.

(29) Chatterjee, R.; Riederer, D. E.; Postawa, Z.; Winograd, N. Coverage-Dependent Molecular Ejection from Ion-Bombarded C_6H_6/Ag{111}. *J. Phys. Chem. B* **1998**, *102*, 4176–4182.

(30) Thompson, M. W. Energy Spectrum of Ejected Atoms During High Energy Sputtering of Gold. *Philos. Mag.* **1968**, *18*, 377–&.

(31) Baxter, J. P.; Singh, J.; Schick, G. A.; Kobrin, P. H.; Winograd, N. Energy and Angle-Resolved Studies of Neutrals Desorbed from Ion Bombarded Polycrystalline Metal-Surfaces. *Nucl. Instrum. Methods Phys. Res., Sect. B* **1986**, *17*, 300–304.

(32) Andersen, H. H.; Johansen, A.; Touboltsev, V. S. The Angular Distribution of Gold Self-Sputtered Under Thermal-Spike Conditions. *Nucl. Instrum. Methods Phys. Res., Sect. B* **2000**, *164*, 727–732.

(33) Dodonov, A. I.; Fayazov, I. M.; Fedorovich, S. D.; Krylova, E. A.; Maskova, E. S.; Molchanov, V. A.; Eckstein, W. Experimental and Computer Study of the Spatial Distributions of Particles Sputtered from Polycrystals. *Appl. Phys. A: Mater. Sci. Process.* **1989**, *49*, 299–304.

(34) Kobrin, P. H.; Schick, G. A.; Baxter, J. P.; Winograd, N. Detector for Measuring Energy-Resolved and Angle-Resolved Neutral-Particle (EARN) Distributions for Material Desorbed from Bombarded Surfaces. *Rev. Sci. Instrum.* **1986**, *57*, 1354–1362.

(35) Willingham, D.; Kucher, A.; Winograd, N. Molecular Depth Profiling and Imaging Using Cluster Ion Beams with Femtosecond Laser Postionization. *Appl. Surf. Sci.* **2008**, *255*, 831–833.

(36) Hrubowchak, D. M.; Ervin, M. H.; Winograd, N. Characterization of Polycyclic Aromatic-Compounds on Surfaces Using Ion-Beam-Induced Desorption and Multiphoton Resonance Ionization. *Anal. Chem.* **1991**, *63*, 225–232.

(37) Meserole, C. A.; Vandeweert, E.; Postawa, Z.; Winograd, N. Internal Excitation Mechanisms of Neutral Atoms and Molecules Emitted from Ion Bombarded Organic Thin Films. *J. Phys. Chem. B* **2004**, *108*, 15686–15693.

(38) Brummel, C. L.; Willey, K. F.; Vickerman, J. C.; Winograd, N. Ion-Beam-Induced Desorption with Postionization Using High Repetition Femtosecond Lasers. *Int. J. Mass Spectrom. Ion Processes* **1995**, *143*, 257–270.

(39) Lu, C.; Wucher, A.; Winograd, N. Molecular Depth Profiling of Buried Lipid Bilayers Using C_{60}-Secondary Ion Mass Spectrometry. *Anal. Chem.* **2011**, *83*, 351–358.

(40) Zheng, L. L.; Wucher, A.; Winograd, N. Depth Resolution During C_{60}^{+} Profiling of Multilayer Molecular Films. *Anal. Chem.* **2008**, *80*, 7363–7371.

(41) Smiley, E. J.; Postawa, Z.; Wojciechowski, I. A.; Winograd, N.; Garrison, B. J. Coarse-Grained Molecular Dynamics Studies of Cluster-Bombarded Benzene Crystals. *Appl. Surf. Sci.* **2006**, *252*, 6436–6439.